SQU Journal for Science, 2019, 24(1), 23-35 DOI: 10.24200/squjs.vol24iss1pp1-23-35
Sultan Qaboos University

Preparation and Characterization of Acidic, Basic and Hydrophobic Dehydrated Carbons and their Capability for Methylene Blue Adsorption

El-Said I. El-Shafey*, Syeda N.F. Ali, Haider Al-Lawati, Saleh N. Al-Busafi

*Department of Chemistey, College of Science, Sultan Qaboos University, P.O. Box 36, PC 123, Al-Khod, Muscat, Sultanate of Oman. *Email: elshafey@squ.edu.om.*

ABSTRACT: Dehydrated carbon (DC) was prepared from date palm leaflets via sulfuric acid treatment. DC was functionalized via amide coupling using ethylene diamine (EDA) and propylene diamine (PDA) to produce basic dehydrated carbons (BDCs): BDC-EDA and BDC-PDA, respectively, and using ethylamine (EA) and aniline (AN) to produce hydrophobic dehydrated carbons (HDCs): HDC-EA and HDC-AN, respectively. Surface areas were found low, between 6.7-16 m^2/g with mesoporosity domination. FTIR shows that –COOH content on DC almost disappeared after surface functionalization. Faster adsorption of methylene blue with larger adsorption capacity was found on HDC-EA than other adsorbents because of stronger hydrophobic interaction forces.

Keywords: Dehydrated carbon; Acidic; Basic; Hydrophobic; Methylene blue.

تحضير وتوصيف الكربون المنزوع المياه الحمضي والقاعدي والكاره للمياه وقدرتهم على إمتزاز الميثيلين الازرق

السعيد إبراهيم الشافعي ، سيده ناهيج فرقان علي ، حيدر اللواتي و صالح البوصافي

الملخص: تم تحضير الكربون منزوع المياه (DC) من سعف النخيل عن طريق المعالجة بحمض الكبريتيك. وقد تم إضافة مجموعات سطحية بواسطة اقتران الأميد مستخدما ايثيلين ثنائي الأميد (EDA) وبروبيلين ثنائي الأميد (PDA) لانتاج الكربون القاعدي منزوع المياه BDC-PDA و-BDC EDA وتم ايضا استخدام أمين الايثيل (EA) والانيلين (AN) لانتاج الكربون الكاره للمياه HDC-EA وHDC-AN . بينت الدراسة أن مساحة سطح الكربون كانت منخفضة وتتراوح بين 6.7 و16 متر^2 /جم وتغلب عليها المسامية المتوسطة. وبينت دراسة الاشعة تحت الحمراء إختفاء مجموعات الكربوكسيل من علي سطح الكربون منزوع المياه (DC) بعد عملية تحوير السطح وظيفيا. وأظهرت الدراسة أيضا أن امتزاز الميثيلين الازرق كان الاسرع والاكثر سعة علي الكربون الكاره للمياه HDC-EA وذلك لوجود قوي تجاذب كارهة للماء.

الكلمات المفتاحية: الكربون المنزوع المياه ، الحمضي ، القاعدي ، الكاره للمياه ، الميثيلين الازرق.

1. Introduction

Sulfuric and phosphoric acids, as dehydrating agents, are capable of carbonizing celluloses and hemicelluloses via the removal of water [1,2]. Hanzawa and Satonaka, in their early studies, prepared chars from raw materials such as filter papers, saw-dust and mandarin orange peel using sulfuric and phosphoric acids [3,4]. The carbon was named as "shitsujunkasseitan" (moistened active charcoal) and later as "suikakasseitan" (hydrated active charcoal) [3,4]. In recent studies, carbon produced by dehydration was called "chemically prepared" [5] or "chemically carbonized" [6] and "dehydrated carbon" [7]. Different agricultural resources have been utilized for the production of dehydrated carbon (DC) using sulfuric acid, including flax shive [8], rice husk [5], peanut shell [9] and date palm leaflets [1,3,10]. Phosphoric acid has also been utilized to produce dehydrated carbon from date palm leaflets [1,11]. Previous studies have shown that DC, prepared by sulfuric acid treatment, is acidic and possesses a high content of acidic functional groups (carboxylic, lactonic and phenolic) with low pH_{zpc} [2,10]. DC is cheaply prepared [10] and due to its high carboxylic content it can be functionalized directly via amide coupling. On the other hand, activated carbon is costive as it requires high energy to prepare and an oxidation step to insert carboxylic groups on its surface before surface functionalization [12].

In this study, DC was prepared from date palm leaflets using sulfuric acid dehydration/oxidation followed by surface functionalization using amines and diamines to produce hydrophobic and basic dehydrated carbons, respectively. DC and functionalized DCs were surface characterized and tested for methylene blue (MB) adsorption in terms of kinetics and equilibrium.

2. Materials and Methods

2.1 Materials

Chemicals used were of analytical grade. Dry date palm leaflets (*Phoenix Dactylifera L.*) were collected from a local farm in Muscat. The leaflets, after cleaning with deionized water, were dried and cut to small pieces (1 cm length) before use in dehydrated carbon preparation.

2.2 Dehydrated carbon preparation and surface functionalization

An amount of 50 g of concentrated sulfuric acid was added dropwise with constant stirring to a mixture of 25 g of clean dry leaflets and ~ 200 ml deionized water. The mixture was left to carbonize at 200 ˚C in an oven for 8 hours. The DC produced was left to cool and residual acid was filtered in a Buchner funnel. The DC was washed several times with deionized water until the wash water showed no change in methyl orange color, indicating that the DC had become acid free. The DC was allowed to dry to constant weight at 120 ˚C. After cooling in a desiccator, it was kept in a well-closed polyethylene jars.

Amide coupling surface functionalization follows a method published earlier for oxidized activated carbon [12]. Ethylene diamine (1,2-diaminoethane), EDA, and propylene diamine (1,3-diamino propane), PDA, were immobilized on the surface of DC to produce basic dehydrated carbons (BDCs) as follows. A mixture of 15 g dry DC and 100 ml of 25 % thionyl chloride in toluene was kept under reflux for 6 hours at 70 ˚C, during which time -COOH groups were converted to -COCl groups. Residual reagents were allowed to evaporate using a rotary evaporator. The sample was dried at 85 ˚C for 2 hours in an oven, followed by reacting with 100 ml (0.75 M) EDA or PDA at 90 ˚C for 24 hours under reflux. On completion of the reaction, nitrogen-containing functional groups were immobilized on the DC surface via amide coupling. For the preparation of hydrophobic dehydrated carbons (HDCs), 15 g of dry DC was allowed to undergo reflux with 200 ml of 50 % thionyl chloride in toluene at 70˚C for 6 hours in a 250 ml round bottomed flask. The product was allowed to cool and the solvents were dried using a rotary evaporator. After evaporation, 100 ml ethylamine (EA) or aniline (AN) were immediately mixed with the carbon and the mixture was left under reflux for 2 hours at 90 ^{o}C. The carbons were purified via soxhlet extraction with 150 ml acetone for 6 hours, followed by washing with deionized water. Residual amines or diamines were removed via washing using 1 M HCl. Another washing using 1 M NaOH was carried out to deprotonate amine groups. Finally, the carbons were washed with deionized water to remove residual base. The carbons were left to dry at 70 ˚C in an oven under vacuum (0.1 atm) until constant weight was obtained. BDCs produced using EDA and PDA are referred as BDC-EDA and BDC-PDA, respectively, and HACs produced using EA and AN are named HDC-EA and HDC-AN, respectively. A schematic illustration for surface functionalization of DC is shown in Figure 1.

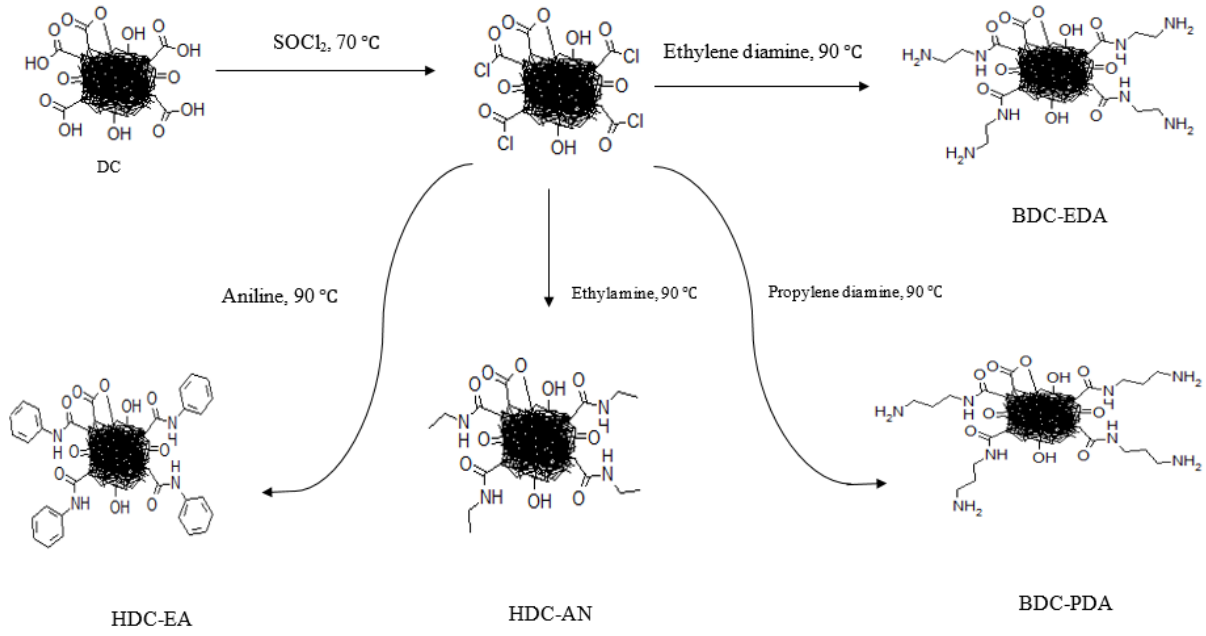

Figure 1. Schematic representation of DC surface functionalization.

2.3 Surface characterization

The surface area of dehydrated carbons was measured using ASAP 2020 (Micrometrics, USA) via nitrogen adsorption at 77 *K* with degassing at 70 ˚C for 24 hours under vacuum. Higher degassing temperature was avoided to prevent possible changes on the carbon surface structure. Apparent density was determined using a standard method [13]. X-ray powder diffraction was conducted using a Philips PW 1830 generator with a Philips PW 1050 powder goniometer (Philips, USA) and copper K_α as the incident radiation. Scanning electron microscopy (SEM) was carried out using a JEOL/EO JSM 5600 with 20 kV accelerating voltage. Using acetanilide as a reference, CHN analysis was carried out using a Euro EA 3000 elemental analyzer (Eurovector, Italy). Infrared analysis was carried out using a FT-IR spectrometer Spectrun BX, Berkin Elmer, (Germany). Surface zero point of charge (pH_{zpc}) was determined following the procedure of Moreno-castilla et al. [14]. Quantification of carboxyl, lactone, phenol and carbonyl groups on the carbon surface was carried out using Boehm titrations [15]. Surface basicity was determined following a method published earlier [12]. Cation exchange capacity (CEC) was determined following the procedure of a standard method [16]. Thermogravimetric analysis was conducted using SDT Q600 Simultaneous DSC-TGA apparatus (TA instruments, USA) under nitrogen in a flow rate of 100 ml/min with a heating rate of 20 ˚C/min from room temperature to 785 ˚C. Zeta potential was determined as a function of pH using a SurPASS^{TM} electrokinetic analyzer (UK) as follows. ~ 0.05 g of carbon was mixed with 0.001 M KCl solution (prepared in CO_2-free water). The pH was adjusted using drops of 0.05 M of NaOH and 0.05 M HCl.

2.4 Adsorption of methylene blue

A stock solution of MB (1000 mg/L) was prepared in deionized water. Standard and test solutions were prepared by suitable dilution in deionized water. Kinetic and equilibrium studies were conducted at 25 ˚C with pH 7.0 as initial pH. Initial pH was adjusted using drops of 0.1 M HCl or 0.1 M NaOH before carbon mixing. In the kinetic study, 0.1 g of carbon was added to 50 ml of MB (100 mg/L) at 25 ˚C. At different periods of time, an aliquot of supernatant was withdrawn for analysis and the adsorption process was followed for ~60 hours under mechanical agitation (100 rpm/min). For the equilibrium study, 0.05 g of carbon was mixed with 25 ml of MB solution (10–700) mg/L at 25 ˚C under mechanical agitation (100 rpm/min) until the equilibrium was reached. Residual MB concentration was determined using a Varian/Cary/50 Conc UV-visible spectrophotometer at λ_{max} 665 nm with deionized water as blank. All the experiments and analysis were carried out at least twice.

3. Results and Discussion

3.1 Surface area and porosity

The adsorption desorption isotherms of nitrogen at 77 K, shown in Figure 2, exhibit characteristics of both Type I and Type IV isotherms according to the classification of Sing et al. [17], but with more dominant characteristics of type IV and a larger extent of mesoporosity [18]. Based on the IUPAC classification, the adsorption isotherms show an H3 hysteresis loop type (Figure 2).

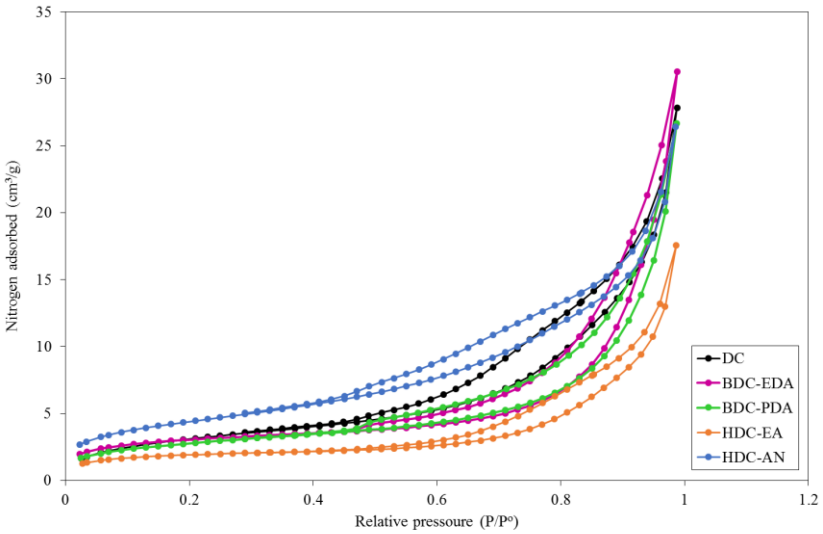

Figure 2. Nitrogen adsorption isotherms at 77 *K* on DC and modified DCs.

Total surface area (S_{BET}) was calculated using the BET equation [19]. According to the Gurvich rule [20], total pore volume (V_t) can be determined from the amount of nitrogen adsorbed at a high relative pressure such as P/P^o= 0.98. Micropore volume (V_{micro}) and mesopore surface area (S_{meso}) were estimated using the *t*-plot method [20] taking

into consideration the theoretical thickness of the adsorbed nitrogen layer (*t*) on carbon black [21] as a reference isotherm (Eq.1). It is more appropriate to use that reference isotherm for carbon-like adsorbents [12,20,22,23].

$$t= 0.88(P/Po)^2 + 6.45(P/Po) + 2.98\ A^o \quad (1)$$

S_{meso} is determined from the slope of the straight line, but V_{micro} is determined from its intercept.

The micropore surface area (S_{micro}) can be determined from Eq. 2 [20,24] while mesopore volume (V_{meso}) can be estimated from Eq. 3, [12,25].

$$S_{micro}= S_{BET} - S_{meso} \quad (2)$$

$$V_{meso} =V_t-V_{micro} \quad (3)$$

(DC)

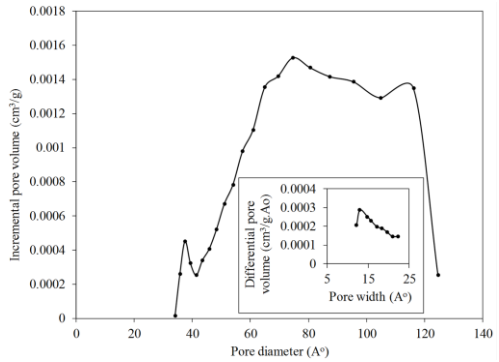

(BDC-EDA)

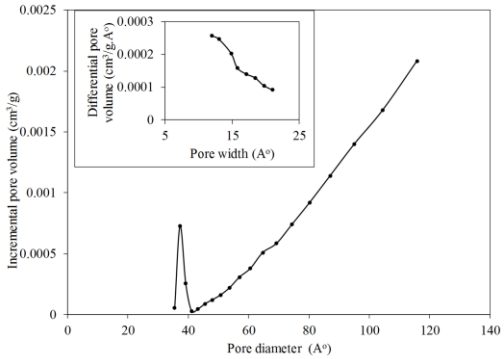

(BDC-PDA)

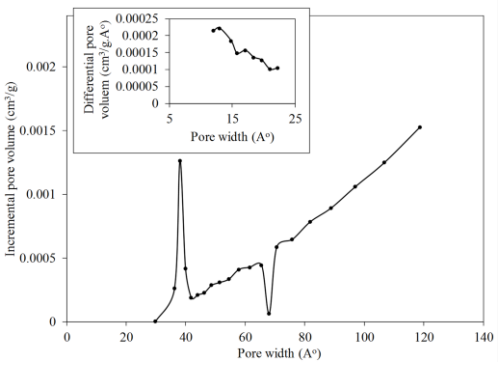

(HDC-EA)

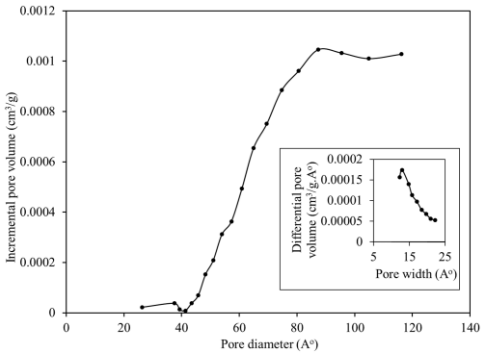

(HDC-AN)

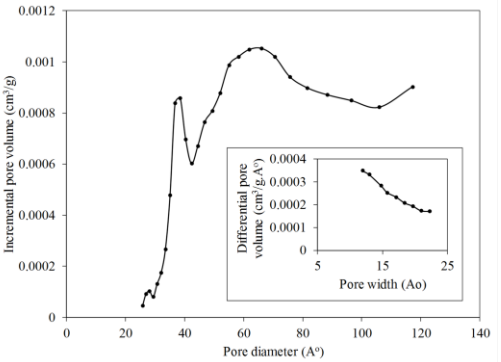

Figure 3. Pore size distribution of DC and functionalized DCs.

Table 1. Surface textural properties of DC and functionalized DCs.

Carbon	S_{BET} (m^2/g)	BET-*C*	V_t (ml/g)	D (A^o)	S_{meso} (m^2/g)	S_{micro} (m^2/g)	V_{micro} (ml/g)	V_{meso} (ml/g)	Apparent density (cm^3/g)
DC	11.55	48.29	0.431	149.1	10.59	0.963	0.0002	0.0428	0.190
BDC-EDA	10.727	270.4	0.0472	176.1	6.985	3.74	0.00164	0.04557	0.254
BDC-PDA	9.884	104.8	0.0319	125.8	8.496	1.388	0.0006	0.0305	0.230
HDC-EA	6.717	308.5	0.0166	98.85	4.74	1.977	0.0009	0.0157	0.290
HDC-AN	15.82	98.21	0.0408	103.3	14.58	1.245	0.0005	0.0403	0.289

During DC preparation, as water evaporates, sulfuric acid concentrates carbonizing the leaflets via the dehydration of cellulose and hemicelluloses with partial fragmentation to lignin and partial oxidation to the surface [8,10]. The surface area of DC and modified DCs is low, as presented in Table 1, unlike activated carbon [12]. Similar low values of surface area were reported previously for dehydrated carbons prepared via sulfuric acid treatment from flax shive (19 m^2/g) [8], rice husk (66 m^2/g) [26] and date palm leaflets (24 m^2/g) [27]. The low surface area of DC is related to the higher content of carbon-oxygen hydrophilic groups that occupy a large fraction of its surface, restricting the adsorption of the non-polar nitrogen molecules [10]. The surface area of BDC-EDA, BDC-PDA and HDC-EA is slightly decreased as a result of surface functionalization. This is probably because the chemically-immobilized chains block, or limit to some extent, the access of nitrogen molecules to some active sites on their surfaces. For HDC-AN, a slight rise in surface area was noticed. The anilide groups on its surface perhaps provided some active sites for nitrogen adsorption. Mesoporosity dominates the surface texture of DC and functionalized DCs (Table 1). In a previous study [12], the surface area of activated carbon was high (823 m^2/g). However, on surface functionalization, it was tremendously decreased [12].

Pore size distribution was investigated using the Barrett–Joyner–Halenda (BJH) model for mesopores and the Horvath–Kawazoe (HK) model for micropores [12,28] showing bimodal pore structure (micro and meso), Figure 3. DC and modified DCs possess different ranges of mesopores with a common peak at ~ 38 A˚ and limited microporosity. As shown in Figure 2, nitrogen adsorption on DC and modified DCs show H3 hysteresis type with no plateau at high P/P˚ values. Thus, V_t values are, to an extent, unreliable [19,20] and thus, the parameters associated with V_t including *D*, V_{meso} and pore size distribution may not be accurate [19,20]. The apparent density is generally low ranging between 0.19 - 0.29 cm^3/g (Table 1).

3.2 X-ray powder diffraction and SEM

The general structure of dehydrated carbons is amorphous, with a common peak at 2θ of 22˚ which can be related to amorphous silica [10,30]. The X-ray diffraction pattern of DC as representative of all DCs is presented in Figure 4. SEM micrographs of carbons (Figure 5) show that DC and modified DCs keep to some extent the fibrous features of the plant morphology with wide pores on their surfaces. The SEM photographic method of identifying pores depends on the sections selected for imaging. In addition, the currently achievable resolution levels make the characterization of most micropores in carbons difficult [29].

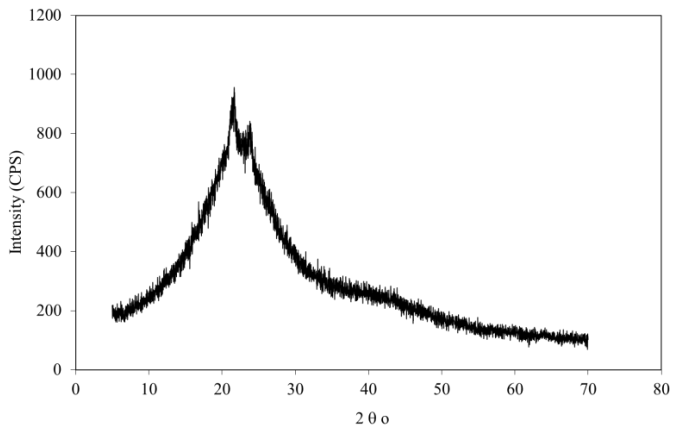

Figure 4. X-ray diffraction of DC.

3.3 FTIR

The broad band between 3400 – 3000 cm^{-1}, Figure 6, for DC corresponds to -OH stretching vibration. Other functionalized DCs show weak and broad bands, in the same region, that can be related to N-H stretching vibrations in

amide and amines on BDCs, and to amide on HDCs. The bands in that region are broad probably because of H-bonding involved among those groups [31].

(DC)

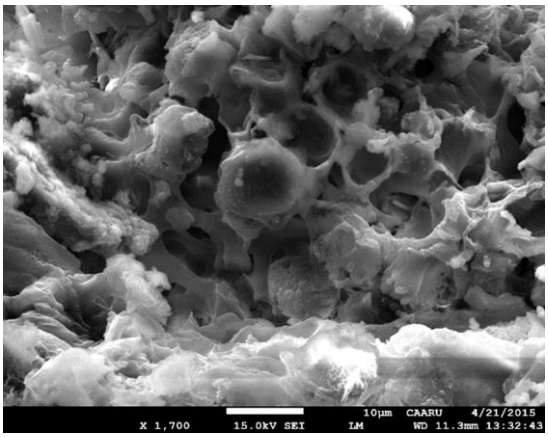

(DC-EDA)

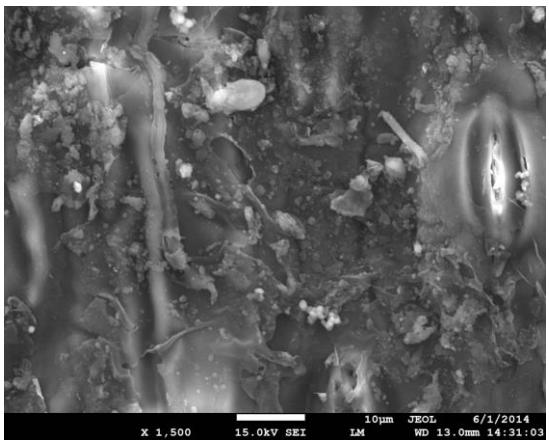

(DC-PDA)

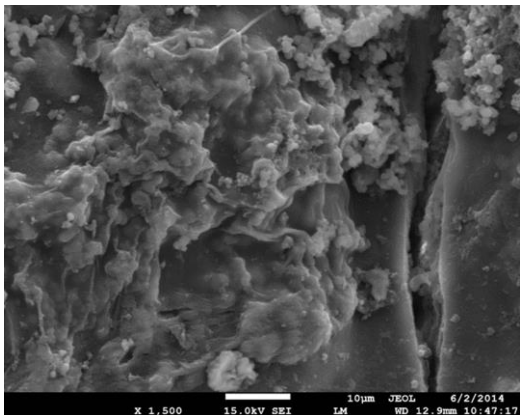

(DC-EA)

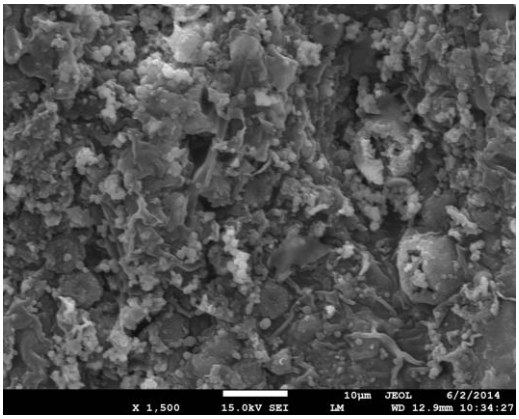

(DC-AN)

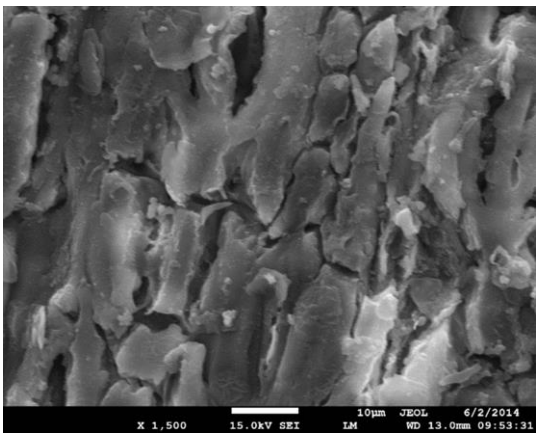

Figure 5. SEM photographs of DC and functionalized DCs.

The bands at 2920 and 2850 cm^{-1} refer to C-H asymmetric and symmetric stretching vibration in the $–CH_2$ group, respectively. A strong band at ~1700 cm^{-1} for DC indicates the presence of $–COO^-$ on its surface. This band almost disappeared for BDCs and HDCs as a result of amide coupling. The bands between 1600-1540 cm^{-1} correspond to C=O and the skeletal C=C aromatic vibrations in all carbons [31]. The band that appears at 1460 cm^{-1} for DC refers to C-H bending vibration for the $–CH_2$ group. The small band that appears around 1440 cm^{-1} for functionalized DCs refers to C−N stretching vibrations in amine and amide groups in BDCs, and amide in HDCs. However, such a band is not

available for DC (Figure 6). The bands between 1400–1000 cm^{-1} are assigned to the O−H bending and C−O stretching vibrations such as phenols, ether, ester and carboxylic acids [31].

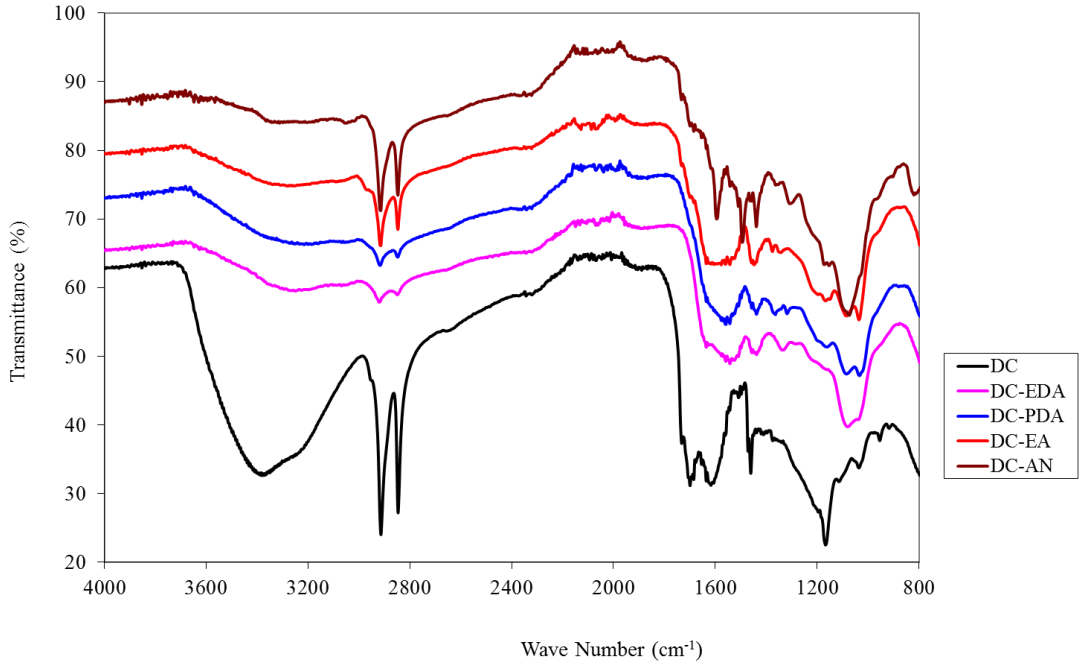

Figure 6. FTIR of DC and functionalized DCs.

3.4 Surface chemical characterization

CHN analysis, presented in Table 2, shows a high content of elemental carbon for DC. However, after surface functionalization, a decrease in carbon content is observed except for HDC-AN. Nitrogen content is higher for BDCs than HDCs and is the minimum for DC. The high nitrogen content on BDCs is attributed to the presence of amide and amine groups immobilized on their surfaces. DC shows more carboxylic and CEC with lower pH_{zpc} than functionalized DCs, indicating the acidic nature of DC (Table 2). Although there is no significant variation of lactone, phenol and carbonyl groups after surface functionalization, the carboxyl content and CEC were clearly decreased by surface functionalization. pH_{zpc} values for BDCs fall within an alkaline range, but for HDCs it is around neutrality (Table 2). BDCs possess more surface basicity than other carbons because of the presence of amine groups immobilized on their surfaces.

Table 2. Surface chemical properties of DC and functionalized DCs.

Carbon	pH_{zpc}	CEC (meq/ 100 g)	Surface functionality (meq/g)				Surface basicity (meq/g)	CHN analysis (%)		
			carboxyl	lactone	phenol	carbonyl		C	H	N
DC	3.24	87.1	2.45	0.23	0.82	1.65	0.36	51.72	4.24	0.52
BDC-EDA	7.7	23.0	0.62	0.21	0.86	1.234	1.52	44.3	4.17	6.15
BDC -PDA	7.6	16.5	0.63	0.23	0.83	0.927	1.9	46.73	4.47	5.82
HDC-EA	7.03	21.4	0.61	0.22	0.81	0.824	0.23	45.71	4.29	3.65
HDC-AN	6.82	26.3	0.62	0.24	0.82	0.88	0.19	64.03	4.22	4.87

As shown in Figure 7, as pH increases, zeta-potential becomes more negative because of OH^- deposition on the carbon surface [32]. The pH of the isoelectric point (pH_{IEP}) for DC is the lowest (~ 3). This is related to the deprotonation of carboxylic groups, which are abundant on DC, and which mainly occur in the pH range of 2-6 [33]. Surface functionalization has led to a decrease in carboxylic group content and accordingly, zeta-potentials of HDCs and BDCs have become less negative than DC. pH_{IEP} shifts to higher values of 6.2, 5.6, 6.5 and 6.8 for HDC-EA, HDC-AN, BDC-EDA and BDC-PDA, respectively (Figure 7). The shifts in pH_{IEP} are related to the decrease in surface acidity.

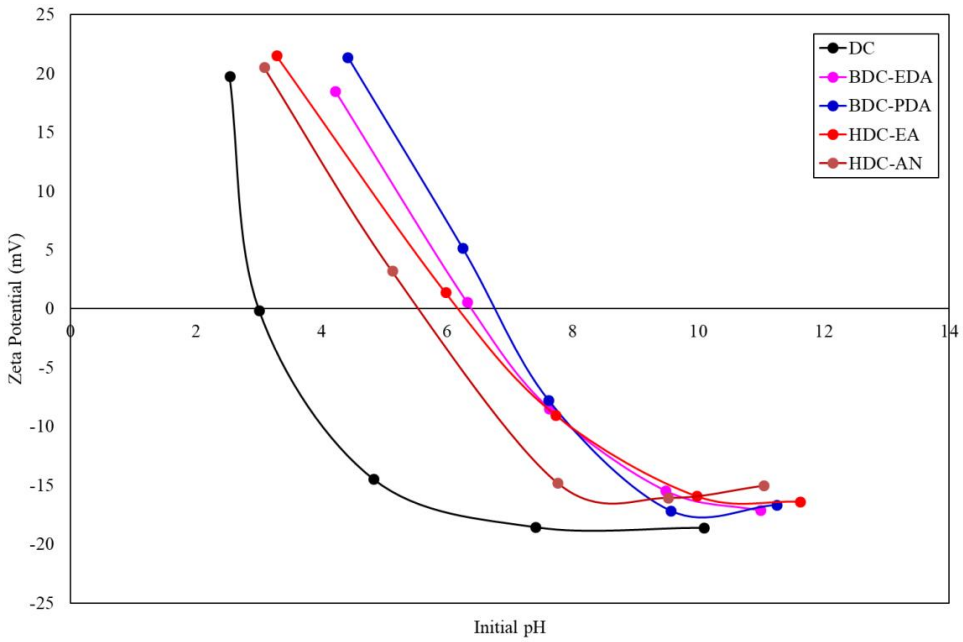

Figure 7. Zeta-potentials of DC and functionalized DCs in 0.001 M KCl solution.

3.5 Thermogravimetric analysis

Figure 8 (A&B) shows the thermogravimetric analysis (TGA) and differential scanning calorimetry (DSC) of carbons, respectively. In the range of 50-150 ˚C, the decrease in wt % is associated with the loss of physisorbed water. The weight loss ranges between 3.6 % for HDC-AN and 8.5 % for DC. DC and BDCs possess higher moisture content than HDCs because of the H-bonding between water molecules and C-O groups on DC, or amine groups on BDCs. HDCs possess less moisture than DC, probably because of their surface hydrophobicity.

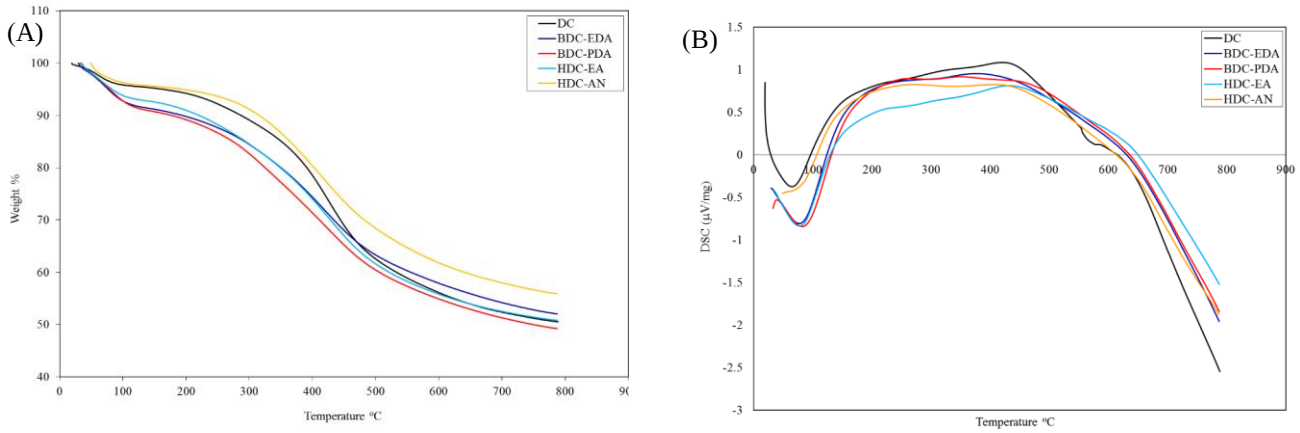

Figure 8. (A) TGA and (B) DSC of DC and functionalized DCs.

Between 150-785 ^{o}C, DC shows a steady weight loss of about 40.7 % with maximum weight loss at 425 ˚C, reaching an overall weight loss of 49.2 % at 785 ˚C. In that temperature range, both CO and CO_2 break away as volatiles [34,35]. CO evolves from the decomposition of carbonyl, ethers, lactone and anhydrides; however CO_2 evolves from the decomposition of carboxylic, lactone and anhydrides [34,35].

Between 250 - 450 ^{o}C, BDC-EDA and BDC-PDA show broad peaks in the range of 250-785 ˚C with maximum weight loss of 40.2 and 43.0 %, respectively. In that temperature range, amide surface groups on both carbons break away [12]. In a previous study, thermal decomposition between 290-310 ˚C was ascribed to amide groups on amide functionalized carbon [36]. Between 250-780 ˚C, a weight loss of 42.7 and 40.5 % was observed for HAC-EA and HAC-AN, respectively, with maximum weight loss taking place between 250 and 450 ˚C. This can be related to the loss of amide functionalities together with CO and CO_2. The relatively high temperature for the decomposition of immobilized functional groups suggests that surface functionalization is of covalent nature [37].

3.6 Methylene blue adsorption

In the kinetic experiment, HDCs and BDCs show the fastest and the slowest MB adsorption, respectively (Figure 9). Pseudo first and pseudo second order kinetic models [38] were tested for the adsorption kinetic data, Equations 4 and 5.

$$Log(q_e\text{-}q_t) = log\ q_e - k_1 t/2.303 \quad (4)$$

$$t/q_t = 1/k_2 q_e^2 + t/q_e \quad (5)$$

where k_1 and k_2 are rate constants for pseudo first and second order models, respectively. q_t is the amount of MB adsorbed per gram of adsorbent (mg/g) at time t. The initial adsorption rate is calculated from k_2 using Eq. 6 [38].

$$h = k_2 q_e^2 \quad (6)$$

The pseudo second order model, presented in Figure 10, better fits the adsorption data with high R^2 values than the pseudo first order model, Table 3, suggesting a mechanism of sharing or exchange of electrons between the carbon surface and MB molecules [38]. The values of k_2 and initial rate h follow the order: HDCs> DC> BDCs (Table 3). The mechanism of interaction of MB with the carbon surface depends mainly on the surface nature of the carbons. HDCs exhibit strong hydrophobic interaction with MB molecules. DC is negatively charged at pH 7 and, thus, interacts with the cationic MB molecules via electrostatic forces. MB adsorption on BDCs involves H-bonding between amine groups on BDCs and MB molecules.

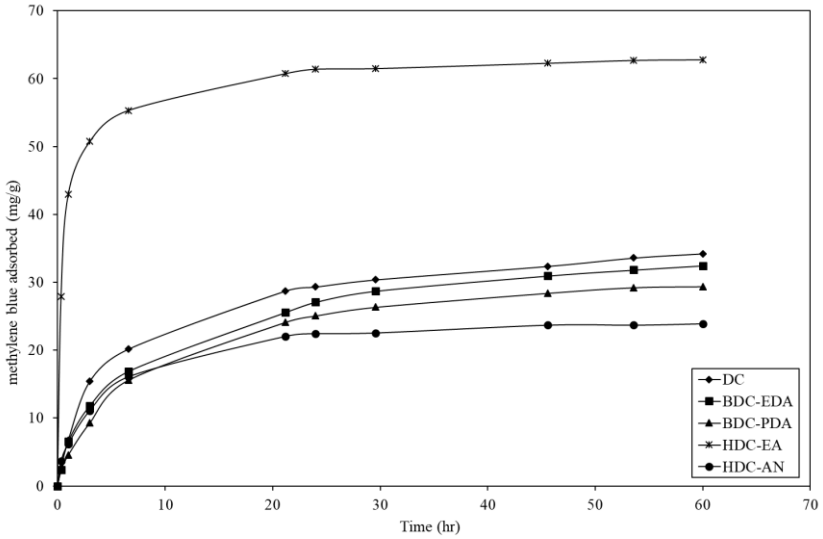

Figure 9. Kinetics of methylene blue adsorption on DC and functionalized DCs at 25 ˚C. (Initial pH 7.0).

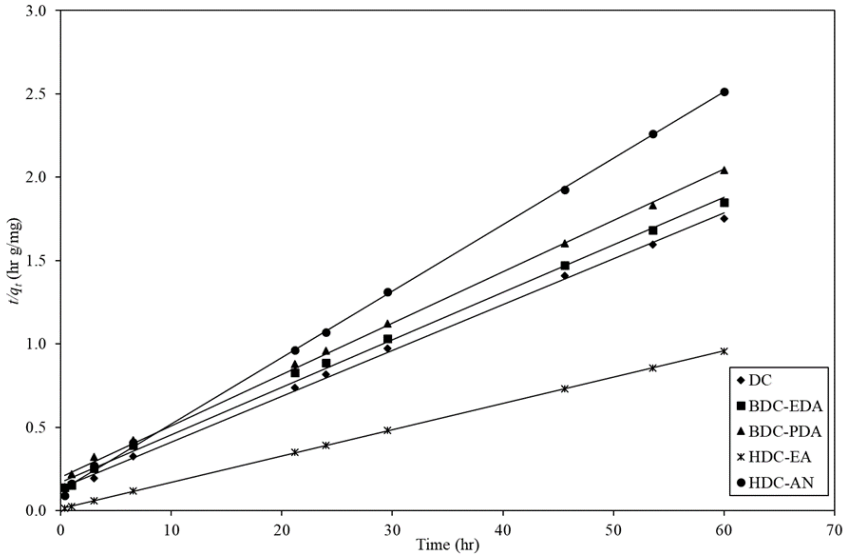

Figure 10. Pseudo second order model application for methylene blue adsorption on DC and functionalized DCs at 25 ˚C. (Initial pH 7.0).

Table 3. Kinetic models' parameters of methylene blue adsorption on DC and functionalized DCs.

Carbon	Pseudo second order model				Pseudo first order model		
	Rate const k_2 (g/mg/hr)	Initial adsorption rate, h (mg/g/hr)	q_e (mg/g)	R^2	k_1 (hr^{-1})	q_e (mg/g)	R^2
DC	0.0056	7.41	36.36	0.9987	0.0912	34.51	0.9144
BDC-EDA	0.0047	5.85	35.09	0.9972	0.0795	32.98	0.9066
BDC-PDA	0.0048	5.01	32.47	0.9982	0.0949	39.78	0.8271
HDC-EA	0.0223	89.3	63.29	0.9999	0.117	36.67	0.9221
HDC-AN	0.0130	8.18	25.13	0.9995	0.0679	21.03	0.9464

Equilibrium adsorption data follow well the L-type adsorption isotherm (Figure 11). The equilibrium adsorption data were tested for the Langmuir and Freundlich equations (Eqs.7and 8).

$$C_e/q_e = 1/b.q + C_e/q \quad (7)$$

$$log\ q_e = log\ K + 1/n\ log\ C_e \quad (8)$$

where K ($L^{1/n}$ $mg^{1-1/n}$ /g) and $1/n$ are Freundich constants which are considered to be relative indicators of adsorption capacity and adsorption intensity, respectively. q and b are the Langmuir constants which are related to the monolayer adsorption capacity (mg/g) and the relative energy of adsorption (L/mg), respectively.

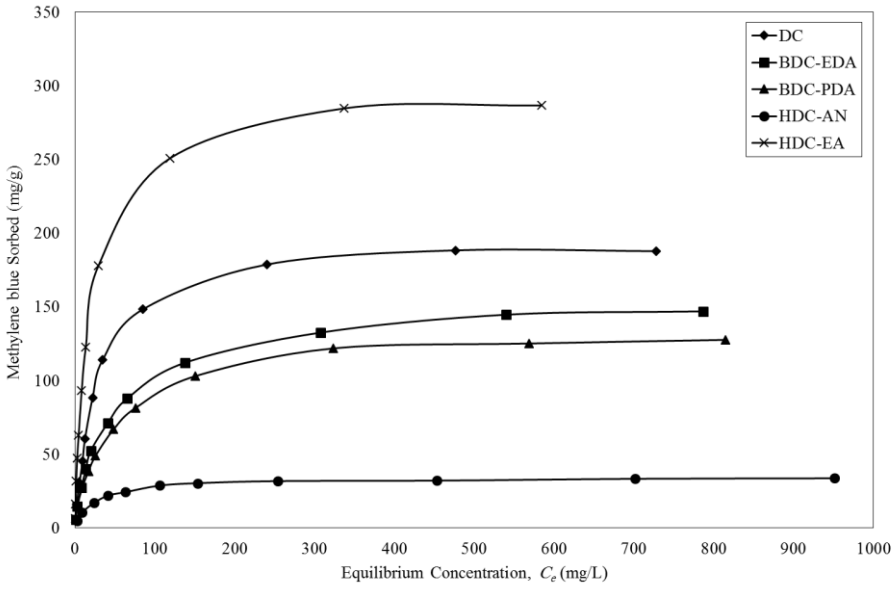

Figure 11. Methylene blue adsorption on DC and functionalized DCs at 25 ˚C. (Initial pH 7.0).

The equilibrium adsorption data better fit the Langmuir model (Figure 12) with high R^2 values than the Freundlich model indicating the formation of a monolayer of MB molecules on carbon surfaces at equilibrium (Table 4). Maximum uptake (q) follows the order: HAC-EA> DC > BDC-EDA > BDC-PDA > HDC-AN.

[39] used a dimensionless factor, R_s, Eq. 9, to indicate the favorability of an adsorption system. R_s is the separation factor which is a direct function of the Langmuir constant b.

$$R_s = 1/(bC_o + 1) \quad (9)$$

R_s values indicate the shape of the isotherm: R_s >1 (unfavorable), R_s = 1 (linear), 1>R_s>0 (favorable) and R_s = 0 (irreversible) [39]. As presented in Table 4, R_s values are all between 0 and 1 indicating 'favorable adsorption'. Strong binding between the MB and HDC-EA, in particular, shows the lowest R_s values. MB adsorption onto the different carbons involves different dominating adsorption forces depending on the nature of the carbons' surfaces. HDC-EA shows the largest MB adsorption capacity involving strong hydrophobic interactions between the ethyl chains on its surface and MB molecules. Although HDC-AN shows a high adsorption rate of MB, its adsorption capacity is the lowest. This is probably due to a steric effect provided by the immobilized anilide groups on HDC-AN [12]. On the

other hand, DC is acidic and negatively charged at pH 7. It adsorbs the MB (cationic dye) dominantly via electrostatic attraction. BDCs probably involves H-bonding (between the amine groups on MB and -NH_2 groups on BDCs surface) and hydrophobic forces involving the ethylene and propylene chains and MB molecules.

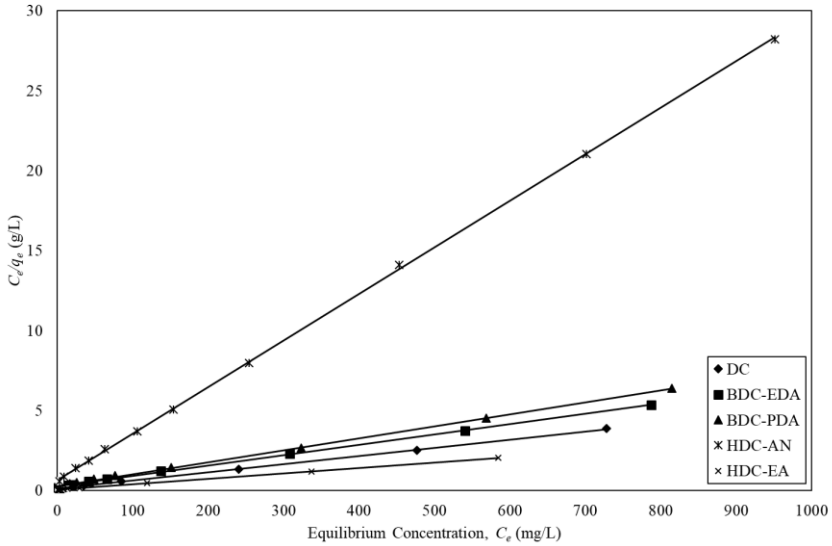

Figure 12. Langmuir adsorption isotherm for the adsorption of Methylene blue on DC and functionalized DCs at 25 ˚C (Initial pH 7).

Table 4. Equilibrium parameters for Methylene blue adsorption on DC and modified DCs.

Adsorbent	Langmuir Constants		Separation factor, R_s	R^2	Freundlich Constants		R^2
	q (mg/g)	b (L/mg)			1/n	K	
DC	196.1	0.0372	0.029-0.73	0.9989	0.482	12.9	0.8803
BDC-EDA	153.8	0.0252	0.038-0.80	0.9989	0.468	9.60	0.9214
BDC-PDA	133.3	0.0262	0.026-0.62	0.9990	0.453	8.99	0.9260
HDC-EA	294.1	0.0626	0.016-0.61	0.9997	0.475	23.8	0.8941
HDC-AN	34.36	0.0447	0.022-0.69	0.9998	0.310	5.40	0.8488

The low surface area of DC and functionalized DCs is not the main factor of MB adsorption. However, the surface chemistry that involves different interaction forces with MB has the most influence on MB adsorption. In our previous study, hydrophobic activated carbon by ethylamine surface area (9.9 m^2/g) showed better performance in MB removal than activated carbon surface area (823 m^2/g) [12]. HDC-EA, in this study (surface area 6.7 m^2/g) shows faster adsorption of MB and larger adsorption capacity (294 mg/g) than activated carbon (surface area 823 m^2/g) with an adsorption capacity of 270 mg/g for MB [12]. In other studies, the adsorption capacity of MB was 47.6 and 126.9 mg/g on activated carbon developed from Ficus carica bast [40] and that developed from biomass waste by H_2SO_4 activation, respectively [41]. The adsorption capacity of MB on activated carbon in those studies is still lower than that of HDC-EA in this study.

4. Conclusion

DC and modified DCs, in this study, possess low surface area. DC is acidic with low pH_{zpc}. The procedure used for surface functionalization to produce BDCs and HDCs is successful as shown from pH_{zpc}, FTIR, TGA and CHN. The dominating interaction forces between methylene blue and carbon surface depend strongly on the nature of carbon surfaces: electrostatic interaction for DC, hydrophobic interaction for HDCs, and hydrogen bonding for BDCs are the dominating forces. Despite the fact that HAC-EA possesses low surface area (by nitrogen adsorption), it shows outstanding performance for methylene blue adsorption. In addition to being cheap to prepare if compared with activated carbon, DC can be functionalized to improve its efficiency for methylene blue removal.

Acknowledgement

The authors would like to thank the Research Council, Sultanate of Oman for funding (RC/SCI/CHEM/2013/01).

References

1. El-Shafey, E.I, Al-Hashmi, A.H.R. Sorption of lead and silver from aqueous solution on phosphoric acid dehydrated carbon. *Journal of Environmental Chemical Engineering*, 2013, **1**, 934-44.
2. El-Shafey, E.I., Al-Lawati, H.A, Al-Saidi, W.S. Adsorption of lisinopril and chlorpheniramine from aqueous solution on dehydrated and activated carbons. *Carbon Letters*, 2016, **19**, 12-22.
3. Hanzawa, M.; Satonaka, S. Crabonization of wood by dehydrating agent. I. Preparation and decolourizing power of hydrated active charcoal from wood. *Research Bulletin of The College Experiment Forests Hokkaido University*, 1955, **17,** 439-463.
4. Hanzawa, M.; Satonaka, S., Crabonization of wood by dehydrating agent. II. Preparation and decolourizing power of hydrated active charcoal from Betula tauschii wood. *Research Bulletin of The College Experiment Forests Hokkaido University*, 1956, **18**, 13-16.
5. El-Shafey, E.I. Removal of Zn(II) and Hg(II) from aqueous solution on a carbonaceous sorbent chemically prepared from rice husk. *Journal of Hazardous Materials*, 2010, **175**, 319-327.
6. El-Shafey, E.I.; Al-Kindy, S.M.Z. Removal of Cu^{2+} and Ag^{+} from aqueous solution on a chemically-carbonized sorbent from date palm leaflets. *Environmental Technol*ogy, 2013, **34**, 395-406.
7. El-Shafey, E.I., Al-Busafi, S., Al-Lawati, H., Al-Shibli, S. Competitive removal of heavy metals from spiked hospital wastewater on acidic and chelating dehydrated carbons. *Separation Science and Technology*, 2016, **51**, 2348-2359.
8. Cox, M., El-Shafey, E.I., Pichugin, A.A., Appleton, Q. Preparation and characterisation of a carbon adsorbent from flax shive by dehydration with sulfuric acid. *Journal of Chemical technology & Biotechnology*, 1999, **74**, 1019-1029.
9. El-Shafey, E.I. Removal of Se(IV) from aqueous solution using sulphuric acid-treated peanut shell. *Journal of Environmental Management*, 2007, **84**, 620-627.
10. El-Shafey, E.I., Al-Lawati, H.A.J., Al-Husaini, A. Adsorption of fexofenadine and diphenhydramine on dehydrated and activated carbons from date palm leaflets. *Chemistry and Ecology*, 2014, **30**, 765-783.
11. El-Shafey, E.I. Immobilization of Hg(II) to Hg(0) on reducing dehydrated carbons. *Journal of Medical and Biomedical Engineering*, 2014, **3**, 292-296.
12. El-Shafey, E.I., Ali, S.N., Al-Busafi, S., Al-Lawati, H.A. Preparation and characterization of surface functionalized activated carbons from date palm leaflets and application for methylene blue removal. *Journal of Environmental Chemical Engineering*, 2016, **4**, 2713-2724.
13. Standard test method for apparent density of activated carbon. *Annual book of ASTM Standards*, 1996, D 2854-96.
14. Moreno-Castilla, C., Lopez-Ramon M.V., Carrasco-Marın F. Changes in surface chemistry of activated carbons by wet oxidation. *Carbon*, 2000, **38**, 1995-2001.
15. Boehm, H.P. Chemical Identification of Surface Groups. In Advances in Catalysis. Academic Press, 1966, **16**, 179-274.
16. Thorpe, A. Collaborative study of the cation exchange capacity of peat materials. *Journal of the Association of Official Analytical Chemists*, 1973, **56**, 154-156.
17. Sing, K.S.W., Everett, D.H., Haul, R.A.W., Moscou, L., Pierotti, R.A., Rouquerol, J., Siemienewska, T. Reporting physisorption data for gas–solid systems, *Pure and Applied Chemistry*, 1985, **57**, 603–619.
18. Giraldo, L., Moreno-Piraján, J.C. Synthesis of activated carbon mesoporous from coffee waste and its application in adsorption zinc and mercury ions from aqueous solution. *E-Journal of Chemistry*, 2012, **9**, 938-948.
19. Thommes, M. Physical adsorption characterization of nanoporous materials. *Chemie Ingenieur Technik*, 2010, **82**, 1059-1073.
20. Lowell, S., Shields, J.E., Thomas, M.A. and Thommes, M. *Characterization of porous solids and powders: surface area, pore size and density*. Springer Science & Business Media, 2012, **16**, 58-254.
21. Standard test method for carbon black- Total and external surface area by nitrogen adsorption, *Annual book of ASTM standards*, 2012, D-6556-01.
22. Miura, K., Yanazawa, H., Nakai, K. The effect of burn-off on the adsorption of N_2 and Ar on a natural graphite. *Adsorption*, 2007, **13**, 139-147.
23. Razdyakonova, G.I., Kokhanovskaya, O.A., Likholobov, V.A. Influence of environmental conditions on carbon Black oxidation by reactive oxygen intermediates. *Procedia Engineering Journal*, 2015, **113**, 43-50.
24. Zhao, C., Liu, L., Zhao, H., Krall, A., Wen, Z., Chen, J., Hurley, P., Jiang, G., Li, Y. Sulfur-infiltrated porous carbon microspheres with controllable multi-modal pore size distribution for high energy lithium–sulfur batteries. *Nanoscale*, 2014, **6**, 882-888.
25. Hesas, R.H., Arami-Niya, A., Daud, W.M.A.W., Sahu, J.N., Preparation and characterization of activated carbon from apple waste by microwave-assisted phosphoric acid activation: application in methylene blue adsorption. *Bioresources*, 2013, **8**, 2950-2966.
26. El-Shafey, E.I. Sorption of Cd(II) and Se(IV) from aqueous solution using modified rice husk. *Journal of Hazardous Materials*, 2007, **147**, 546-555.

27. El-Shafey, E.I.; Al-Lawati, H.; Al-Sumri, A.S. Ciprofloxacin adsorption from aqueous solution onto chemically prepared carbon from date palm leaflets. *Journal of Environmental Science*, 2012, **24**,1579-1586.
28. Gregg, S.J. and Sing, K.S.W. Adsorption, surface area and porosity, 2nd ed., Academic Press, London, UK, 1982.
29. Achaw, O.W. A study of the porosity of activated carbons using the scanning electron microscope. In *Scanning Electron Microscopy*, INTECH, 2012, Chapter **24**, 473-490.
30. Mopoung, S. Surface image of charcoal and activated charcoal from banana peel. *Journal of the Microscopy Society of Thailand*, 2008, **22**, 15-19.
31. Gómez-Serrano, V., Acedo-Ramos, M., López-Peinado, A.J., Valenzuela-Calahorro, C. Oxidation of activated carbon by hydrogen peroxide. Study of surface functional groups by FT-i.r. *Fuel*, 1994, **43**, 387-395.
32. Lu, C., Chiu. H., Liu, C., Removal of zinc (II) from aqueous solution by purified carbon nanotubes: kinetics and equilibrium studies. *Industrial Engineering Chemistry Research*, 2006, **45**, 2850-2855.
33. Harry, I.D., Saha, B., Cumming, I.W. Effect of electrochemical oxidation of activated carbon fiber on competitive and noncompetitive sorption of trace toxic metal ions from aqueous solution. *Journal of Colloid and Interface Sci*ence, 2006, **304**, 9-20.
34. Moreno-Castilla, C., Ferro-Garcia, M.A., Joly, J.P., Bautista-Toledo, I., Carrasco-Marin, F., Rivera-Utrilla, J. Activated carbon surface modifications by nitric acid, hydrogen peroxide, and ammonium peroxydisulfate treatments. *Langmuir*, 1995, **11**, 4386-4392.
35. Figueiredo, J.L., Pereira, M.F.R., Freitas, M.M.A., Orfao, J.J.M. Modification of the surface chemistry of activated carbons. *Carbon*, 1999, **37**, 379-1389.
36. Niyogi, S., Bekyarova, E., Itkis, M.E., McWilliams, J.L., Hamon, M.A, Haddon, R.C. Solution properties of graphite and grapheme. *Journal of the American Chemical Society*, 2006, **128**, 7720-7721.
37. Collins, W.R., Lewandowski, W., Schmois, E., Walish, J., Swager, T.M. Claisen rearrangement of graphite oxide: a route to covalently functionalized graphenes. *Angewandte Chemie-International Edition*, 2011, **123**, 9010-9014.
38. Ho, Y.S., Mckay, G. Sorption of dye from aqueous solution by peat. *Chemical Engineering Journal*, 1998, **70**, 115-124.
39. Hall, K.R., Eagleton, L.C., Acrivos, A., Vermeulen, T. Pore-and solid-diffusion kinetics in fixed-bed adsorption under constant-pattern conditions. *Industrial & Engineering Chemistry Fundamentals*, 1966, **5**, 212-223.
40. Pathania, D., Sharma, S., Singh, P. Removal of methylene blue by adsorption onto activated carbon developed from Ficus carica bast. *Arabian Journal of Chemistry*, 2017, **10**, 1445-1451.
41. Jawad, A.H., Rashid, R.A., Ishak, M.A.M., Wilson, L.D., 2016. Adsorption of methylene blue onto activated carbon developed from biomass waste by H_2SO_4 activation: kinetic, equilibrium and thermodynamic studies. *Desalination and Water Treatment*, 2016, **57**, 25194-25206.

Received 17 September 2018
Accepted 5 February 2019